American Journal of Energy Engineering
2014; 2(5): 108-126
Published online November 10, 2014 (http://www.sciencepublishinggroup.com/j/ajee)
doi: 10.11648/j.ajee.20140205.12
ISSN: 2329-1648 (Print); ISSN: 2329-163X (Online)

Single and multicomponent droplet models for spray applications

Shah Shahood Alam[1], Ahtisham Ahmad Nizami[1], Tariq Aziz[2]

[1]Pollution and Combustion Engineering Lab. Department of Mechanical Engineering, Aligarh Muslim University, Aligarh-202002, U.P. India
[2]Department of Applied Mathematics, Aligarh Muslim University, Aligarh-202002, U.P. India

Email address:
sshahood2004@yahoo.co.in (S. S. Alam)

To cite this article:
Shah Shahood Alam, Ahtisham Ahmad Nizami, Tariq Aziz. Single and Multicomponent Droplet Models for Spray Applications. *American Journal of Energy Engineering*. Vol. 2, No. 5, 2014, pp. 108-126. doi: 10.11648/j.ajee.20140205.12

Abstract: An unsteady, spherically symmetric, single component, diffusion controlled gas phase droplet combustion model was developed first, by solving numerically the time dependent equations of energy and species. Results indicated that flame to droplet diameter ratio (flame standoff ratio) increased throughout the droplet burning period, its value being much smaller than that of the quasi-steady case, where it assumes a large constant value. Effects of fuels on important combustion characteristics suggested that combustion parameters were influenced primarily by the fuel boiling point. Droplet mass burning rate variation was smallest for ethanol in comparison with methyl linoleate (biodiesel) and n-heptane. Also, effects of fuels on CO, NO, CO_2, and H_2O concentrations were determined from the point of view of getting a qualitative trend.For multicomponent spherical combustion of a heptane-dodecane droplet, it was observed that the mass fraction of heptane decreased abruptly to a minimum value as the droplet surface was approached. For a 200μm hexane-decane droplet (at its boiling point), vaporising in conditions of 1 atm and 1000K with $Le_l = 10$, it was observed that mixing of air and fuel vapour resulted in a higher concentration of hexane at the droplet surface at the end of droplet lifetime thereby altering the vaporisation behaviour. Other conditions remaining same, an increase in Lewis number resulted in a higher mass fraction of hexane being present at the droplet surface. A detailed multicomponent (MC) droplet vaporisation model (diffusion limit model with convection and no internal liquid circulation) was also evolved by numerically solving the transient-diffusive equations of species and energy for a 280 μm (heptane-dodecane) droplet vaporising at 1 atm and 1000 K with Re_σ=100, and Le_l= 10. The present MC model was compared with other existing models and was found to be simpler and quite accurate. The submodels developed in the present work can be implemented in spray analysis.

Keywords: Single and Multi-Component Droplet Models, Numerical Technique, Simplified Approach, Different Fuels, Spray Combustion Application

1. Introduction

The subject of 'Liquid Droplet Combustion' serves as the basic step for understanding the complex process of spray combustion prevalent in diesel engines, industrial boilers and furnaces, liquid rockets and gas turbines. In these devices, liquid fuels are atomised into fine sprays, in order to increase the surface area per volume so as to promote evaporation.

An isolated droplet combustion under microgravity (near zero gravity) condition is an ideal situation for studying liquid droplet combustion phenomenon. It leads to a simplified, one dimensional solution approach of the droplet combustion model' (a spherical liquid fuel droplet surrounded by a concentric, spherically symmetric flame).

For the present work, different droplet evaporation/combustion models are evolved with respect to single/pure component and multicomponent fuels. At first, a comprehensive, single component, spherically symmetric gas phase droplet combustion model is developed and tested for important combustion and emission characteristics. After that, simplified droplet vaporisation and combustion models are developed followed by a more detailed multicomponent droplet vaporisation model. The results obtained are compared with the existing experimental/modelling results of other authors for the same conditions.

Some noteworthy contributions related to single component, spherically symmetric, liquid droplet combustion are mentioned below. Kumagai and co-workers [1,2,3] were pioneers in conducting spherically symmetric

droplet combustion experiments in microgravity conditions through drop towers, capturing the flame movement and further showed that F/D (also called flame standoff ratio) increases throughout the droplet burning history, thereby signifying that droplet combustion is transient phenomenon.

Waldman [4] and Ulzama and Specht [5] used analytical procedure whereas Puri and Libby [6] and King [7] employed numerical techniques in developing spherically symmetric droplet combustion models. The results of these authors were mainly confined to the observations that unlike quasi-steady case, flame is not stationary and flame to droplet diameter ratio increases throughout the droplet burning period.

A study on convection was carried out by Yang and Wong [8] who investigated the effect of heat conduction through the support fibre on a droplet vaporising in a weak convective field. Another aspect related to convection is the presence of internal circulation within the droplet. Law, C.K [9] introduced the 'infinite diffusivity' or 'batch distillation' model which assumed internal circulation within the droplet. Droplet temperature and concentrations were assumed spatially uniform but temporally varying. It was suggested that the more volatile substance will vaporise from the droplet surface leaving only the less volatile material to vaporise slowly.

In the absence of internal circulation, the infinite diffusivity model was found to be inappropriate. For such conditions Landis and Mills [10] carried out numerical analysis to solve the coupled heat and mass transfer problem for a vaporising spherically symmetric, miscible bicomponent droplet. This model in literature is termed as 'diffusion limit' model.

Law, C.K [11] generalised the formulation of Landis and Mills and suggested that regressing droplet surface problems are only amenable to numerical solutions. Tong and Sirignano [12] devised a simplified vortex model which required less computing time than the more detailed model of Lara-Urbaneja and Sirignano [13].

In an experimental investigation, Aldred et al. [14] used the steady state burning of n-heptane wetted ceramic spheres for measuring the flame structure and composition profiles for the flame corresponding to 9.2 mm diameter sphere. Their results indicated that oxidizer from the ambient atmosphere and fuel vapour from the droplet surface diffuse towards each other to form the flame where the products of combustion are formed and the flame temperature is highest.

Marchese and Dryer [15] considered detailed chemical kinetic modelling for the time dependent burning of isolated, spherically symmetric liquid droplets of methanol and water using a finite element chemically reacting flow model. It was noted that a favourable comparison occurred with microgravity droplet tower experiment if internal liquid circulation was included which could be caused by droplet generation/deployment techniques. However, significant deviations from the quasi-steady d^2-*law* were observed.

A liquid composed of a multitude of chemical species is called a multicomponent (MC) liquid. The overwhelming majority of liquids used for power production are MC liquids; these include gasoline, diesel fuel and kerosene.

Much of the earlier studies on droplet combustion used pure fuels. Multicomponent effects were not considered to be serious for the reason that the requirements of combustor efficiency and emission were generally not stringent. A review of the existing literature reveals that multicomponent droplet studies constitute only a relatively small fraction of the available literature.

However, recent developments in engine design and fuel formulation indicate that multicomponent effects will become progressively more important in the utilisation of liquid fuels. Combustion processes within engine will be more tightly controlled to further improve efficiency and reduce emissions.

The impetus for continued research in this field comes from the search for alternative sources of fuel like vegetable oils and better ways of fuel utilisation in the face of increasing demand and dwindling oil reserves. Also of major concern are the problems of combustion related pollution and the use of combustion for disposal of hazardous wastes. In the process, fuels developed are blends of several components.

There also exists considerable interest in the utilisation of such hybrid fuels as water/oil emulsions, alcohol/oil solutions and emulsions, and coal/oil mixtures. The widely different physical and chemical properties of the constituents of these hybrid fuels necessitate consideration of multicomponent effects in an essential way.

To understand heterogeneous multicomponent fuel combustion either as a droplet or in some other form (e.g. pool burning), the following factors have to be considered:

The relative concentrations and volatility of the liquid constituents, as would be expected. The miscibility of the liquid constituents. This controls the phase change characteristics**.** The internal circulation which influences the rate with which the liquid components can be brought to the surface where vaporisation takes place.

Liquid phase mass diffusion is much slower than liquid phase heat diffusion so that thin diffusion layers can occur near the surface, especially at high ambient temperatures at which the surface regression rate is large. The more volatile substances tend to vaporise faster at first until their surface concentration values are diminished and further vaporisation of those quantities becomes liquid phase mass diffusion controlled [16].

It is then obvious that not only the fuel vaporisation process, but also strongly kinetically dependent gas phase combustion phenomena such as ignition, extinction and pollution formation will depend sensitively on composition of the liquid fuel and how its vaporisation is modelled [17].

These differences have been attributed to transient liquid mass transport in the droplet interior, volatility differential between the constituent fuels, phase equilibrium at the droplet surface, and thermo transport properties that are functions of mixture compositions, temperature and pressure [18].

Here, different components vaporise at different rates, creating concentration gradients in the liquid phase and causing liquid phase mass diffusion. The theory requires coupled solutions of liquid phase species continuity equations, multicomponent phase-equilibrium relations, typically Roult's law and gas phase multicomponent energy and species continuity equations [19].

Feeling a need for an analytical solution, Law and Law [17] derived a simplified approximate analytical solution for quasi-steady, spherically symmetric, liquid phase mass diffusion controlled vaporisation and combustion of multicomponent fuel droplets for the case where liquid phase species diffusion was slow compared to droplet surface regression rate. An ideal solution behaviour was assumed.

A unique feature of the diffusion dominated droplet vaporisation mechanism was the possible attainment of approximately steady state temperature and concentration profiles within the droplet, which then led to a steady state vaporisation rate. Based on this concept, Law and Law [17] formulated a d^2-*law* model for multicomponent droplet vaporisation and combustion. It was noted that, the mass flux fraction or the fractional vaporisation rate ε_m was propotional to the initial liquid phase mass fraction of that species prior to vaporisation.

Their solution allowed direct evaluation of all combustion properties of interest, including the liquid phase composition profiles, once the droplet surface temperature was determined iteratively. Therefore utilisation of the their multicomponent d^2-*law* is almost as simple as the classical pure component d^2-*law*.

Tong and Sirignano [12] analysed the problem of transient vaporisation of a multicomponent droplet in a hot convective environment. The model accounted for the liquid phase internal circulation and quasi-steady, axisymmetric gas phase convection. Essentially it was called the simplified vortex model for the liquid phase (which was basically a diffusion limit model with axisymmetry rather than spherical symmetry) and a simplified, quasi-steady, axisymmetric convective model for the gas phase.

The objective of the study were (i) to develop an algorithm for multicomponent droplet vaporisation simple enough to be feasibly incorporated into a complete spray combustion analysis and yet be accountable for important physics, (ii) comparison of the developed model with existing models, and (iii) to compare the different models with the available experimental data.

Lerner et al. [20] conducted experiments for measuring overall vaporisation rates, droplet composition and droplet trajectories for free, isolated, bicomponent paraffin droplets subjected to large relative gas-droplet velocities. The experimental results for bicomponent fuel droplets of heptane and dodecane vaporising at atmospheric pressure were used for comparison with other theoretical models of Tong and Sirignano [12].

Aggarwal et al. compared different evaporation models for their feasibility in spray calculations [21].

Shaw, B.D [22] investigated spherically symmetric combustion of miscible droplets for the case where liquid phase species transport was slow relative to droplet surface regression rates. Attention was focussed on later periods of combustion, following decay of initial transients, when droplet species profiles change slowly relative to droplet size changes and d^2-*law* combustion closely holds.

Spherical combustion of heptane-dodecane droplet was considered at one atmosphere and 300 K. Asymptotic analysis was employed. The gas phase was assumed to remain quasi-steady. Properties were not calculated as a function of temperature. A concentration boundary layer where species profile changed sharply in the radial coordinate was shown to be present at the droplet surface.

Mawid and Aggarwal [23] numerically analysed transient combustion of a spherically symmetric 50-50 by mass heptane-decane liquid fuel droplet. The unsteady effects caused by the liquid and gas phase processes were considered and were divided into three main periods.

An important aspect of multicomponent droplet combustion is the c*ombustion of chlorinated hydrocarbons, dealing with the effects of chlorination and blending.* Direct incineration is a promising technology for the disposal of hazardous wastes with the potential of complete detoxification. Many hazardous wastes are chlorinated hydrocarbons (CHC_S) which are incineration resistant

A comprehensive experimental investigation was conducted [24] to quantify the combustion characteristics of pure CHC_S as well as their mixtures with regular hydrocarbon fuels, with the specific interest of enhancing the incinerability of CHC_S through judicious blending with hydrocarbon fuels.

Mixtures of TECA (1,1,2,2,-tetrachloroethane) and various alkanes were studied to determine the role of volatility differentials in the burning of TECA.

It was observed that the incineration of a heavily chlorinated hydrocarbon could be promoted through the addition of a small quantity of a less volatile regular hydrocarbon fuel, and emphasized the importance of developing rational blending strategies in the incineration of hazardous wastes.

Another important aspect of multicomponent droplet burning is vaporisation *of alcohols with respect to the water vapour condensation phenomenon.* Some previous studies on the light alcohols, namely methanol and ethanol, have suggested that the droplet vaporisation rate can be substantially enhanced through condensation of water vapour from the environment.

That is because the saturation temperatures of ethanol and methanol are lower than that of water and because they are also completely water miscible, water vapour from a humid environment could condense onto and subsequently dissolve into the relatively cool alcohol droplet. The condensation heat release could be used by alcohol for its own vaporisation, thereby facilitating its evaporation rate [25].

An interesting phenomenon accompanying multi-component droplet combustion i*s microexplosion*. Microexplosion (frag-mentation of liquid droplets due to

violent internal vaporisation) has potential in improving engine performance since it can be used to promote the atomisation of heavy fuels by adding certain amounts of light fuels.

Zeng and Lee [26] presented a numerical model of microexplosion for multicomponent droplets. The first part of the model addressed the mass and temperature distribution inside the droplet and the bubble growth within the droplet. The bubble generation was described by a homogeneous nucleation theory, and the subsequent bubble growth led to the final explosion i.e. break up.

The second part of the model determined when and how the break up process proceeded. Unlike adhoc/empirical approaches reported in the literature, the size and velocity of sibling droplets (secondary droplets) were determined by a linear instability analysis.

The vaporisation behaviour of an oxygenate diesel blend was analysed at the end. It was found that microexplosion was possible under typical diesel engine environments for this type of fuel. Occurrence of microexplosion shortened the droplet lifetime, and this effect was stronger for droplets with larger sizes or a near 50/50 composition.

2. Selection of Fuels

The selected fuels included alkanes, alcohols and biodiesels. In addition to pure fuels, like n- heptane, ethanol and biodiese fuel methyl linoliate, mixtures of n-heptane-n-dodecane and n-hexane-n-decane were considered in the multi-component droplet analysis.

These family of fuels have different thermophysical and transport properties and structure. Therefore variation in their properties should affect combustion characteristics like flame temperature, flame radius, transfer number, burning constant, burning rate, combustion lifetime, flame to droplet diameter ratio as well as emission characteristics. n-heptane is used as a test fuel in many experimental and theoretical studies and therefore lot of experimental and modelling data are available for comparison purposes. Some experimental and theoretical studies used n-heptane for sooting , since it is a sooting fuel.

For the combustion of liquid fuels, it is convenient to express the composition in terms of a single hydrocarbon, even though it is a mixture of many hydrocarbons (multicomponent fuel) [27].

Thus gasoline is usually considered to be octane and diesel fuel is considered to be dodecane. n-octane and n-dodecane are important fuels for experimental and modelling studies. Methanol has relatively simple gas chemistry making it more suitable to theoretical treatment, it is also a non sooting fuel.

Ethanol is regaining its popularity for use in practical applications. The Clean Air Act Amendments of 1990 mandated the use of oxygenated fuels such as ethanol and methanol in regions of country experiencing high levels of CO [28]. In India, Ministry of Petroleum and Natural Gas launched a nationwide “Ethanol Blended Petrol Program” in 2006 as a step towards gradually reducing the dependence on fossil fuels and increasing the use of alternative fuels that are renewable in nature.

Blending of ethanol with diesel fuels helps in reducing the amount of aromatic precursors such as acetylene that lead to a drastic suppression of polycyclic aromatic hydrocarbons (PAHs) / soot formation [28].

Biodiesel is a substitute for petroleum diesel and can be used in diesel engines with minor modifications. Indian government has set up a biofuel board to promote its cultivation on a large scale. Biodiesel is methyl or ethyl ester of fatty acid made from virgin or used vegetable oils (both edible and non edible) and animal fat. The main resources for biodiesel production can be non edible oils obtained from plant species such as Jatropha curcas (Ratanjyot), Pongamia pinnata (Karanj), Calophyllum inophyllum (Nagchampa) etc. [29].

As evident from the available literature on biodiesels regarding their structure, nearly all biodiesels are made up of a combination (in different percentages) of either Linoleic acid (Methyl linoleate), Oleic acid (Methyl oleate) or Stearic acid (Methyl stearate). Out of these, Safflower oil contains about 78.0 % Methyl linoleate; Sunflower oil contains about 74 % methyl linoleate; karanj 44.5-71.3 % Methyl oleate and 10.8-18.3 % Methyl Linoleate; Rice-bran 26.4-35.1 % Methyl linoleate, 39.2-43.7 % Methyl oleate; Neem 49.1-61.9 % Methyl oleate, 2.3-25.8 % Methyl linoleate, 14.4-24.1 % Methyl stearate [30]; while Jatropha about 34.3 % Methyl oleate, 43.12 % Methyl linoleate and 7.46 % Methyl stearate. For high percentage of a particular methyl ester in a biodiesel, the behaviour of that biodiesel with regards to combustion and emission characteristics can be predicted by considering it as a pure or single component fuel made up of that particular methyl ester.

It should be added that at present relatively less amount of thermophysical and transport data of biodiesel fuels exists in the literature. Also, combustion and emission data of biodiesels with respect to single droplet is limited. One of the motivation factor for the present work was to overcome this deficiency.

The succeeding paragraph describes methods of estimating properties of biodiesel fuel based on their chemical composition and structure at specified temperature and pressure, used in combustion modelling for the present work. Biodiesel contains six or seven fatty acid esters. It is possible to estimate the properties of each pure component and then compute the mixture properties based on some mixing rules [31]. Further, in the formulation of biodiesel fuel, there is an advantage over petroleum that the chemistry of the components is well defined. The fuel is an ester of fatty acids derived from natural sources. As a result fatty acids present in significant quantity are palmitic acid, stearic acid, oleic acid, linoleic acid, linolenic acid and erucic acid. Relative composition change by sources, but the components do not [32].

Once properties of one of the major components is estimated, the same methodology can be applied for other components.

2.1. Properties Etimation for Biodiesel Fuel (Methyl Linoleate)

The critical properties are an important starting point as they are used to estimate other important thermodynamic properties. For the present work, critical properties of fatty acid methyl esters of pure vegetable oils were estimated by two widely used methods: Joback modification of Lydersen's method, and Ambrose's method, since these two methods were previously shown to be able to provide reasonably accurate estimates for most compounds. Thermophysical properties of chosen fuels are given in Table 1.

On comparing with reported values [31,33], slight discrepancy (10-12%) was found with normal boiling point temperature as calculated in the present work. The reason may be that we have used chemical structure as the basis for estimation whereas Yuan et al.[31] have used different correlations for determing the normal boiling point. For comparison of critical data with the reported results [31], it was observed that there was a very good agreement with respect to critical pressure and critical molar volume (Table 2), however critical temperature values differ since for the present work, the calculation for the critical temperature involves the normal boiling point, hence the variation. Once these properties were known, they were used in turn for determining combustion parameters like transfer number B_T, burning constant k_b, droplet lifetime t_d and thermal diffusivity α_g.

3. Problem Formulation

3.1. Development of Spherically Symmetric, Single Component, Droplet Combustion Model for the Gas Phase

Following assumptions are invoked:

Spherical liquid fuel droplet is made up of single chemical species and is assumed to be at its boiling point temperature surrounded by a spherically symmetric flame, in a quiescent, infinite oxidising medium with phase equilibrium at the liquid-vapour interface expressed by the Clausius-Clapeyron equation.

Droplet processes are diffusion controlled (ordinary diffusion is considered, thermal and pressure diffusion effects are neglected). Fuel and oxidiser react instantaneously in stoichiometric proportions at the flame. Chemical kinetics is infinitely fast resulting in flame being represented as an infinitesimally thin sheet.

Ambient pressure is subcritical and uniform. Conduction is the only mode of heat transport, radiation heat transfer is neglected. Soret and Dufour effects are absent.

Thermo physical and transport properties are evaluated as a function of pressure, temperature and composition. Ideal gas behaviour is assumed. Specific enthalpy 'h' is a function of temperature only. The product of density and diffusivity is taken as constant. Gas phase Lewis number Le_g is assumed as unity.

The overall mass conservation and species conservation equations are given respectively as:

$$\frac{\partial \rho}{\partial t}+\frac{1}{r^2}\frac{\partial}{\partial r}\left(r^2 \rho v_r\right)=0 \tag{1}$$

$$\frac{\partial (\rho Y)}{\partial t}+\frac{1}{r^2}\frac{\partial}{\partial r} r^2\left[\rho v_r Y-\rho D\frac{\partial Y}{\partial r}\right]=0 \tag{2}$$

Where;

t is the instantaneous time

r is the radial distance from the droplet center

ρ is the density

v_r is the radial velocity of the fuel vapour

D is the mass diffusivity

Y is the mass fraction of the species

equations (1) and (2) are combined to give species concentration or species diffusion equation for the gas phase as follows

$$\frac{\partial Y}{\partial t}=D_g\frac{\partial^2 Y}{\partial r^2}+\frac{2D_g}{r}\frac{\partial Y}{\partial r}-v_r\left(\frac{\partial Y}{\partial r}\right) \tag{3}$$

D_g is the gas phase mass diffusivity

The relation for energy conservation can be written in the following form

$$\frac{\partial (\rho h)}{\partial t}+\frac{1}{r^2}\frac{\partial}{\partial r}\left[r^2\rho\left(v_r\cdot h-D.\,C_p\frac{\partial T}{\partial r}\right)\right]=0 \tag{4}$$

The energy or heat diffusion equation for the gas phase, equation (5) can be derived with the help of overall mass conservation equation (1) and equation (4), as:

$$\frac{\partial T}{\partial t}=\alpha_g\frac{\partial^2 T}{\partial r^2}+\frac{2\alpha_g}{r}\frac{\partial T}{\partial r}-v_r\left(\frac{\partial T}{\partial r}\right) \tag{5}$$

T is the temperature, α_g is gas phase thermal diffusivity. Neglecting radial velocity of fuel vapour v_r for the present model, equations (3) and (5) reduce to a set of linear, second order partial differential equations (equations 6 and 7).

$$\frac{\partial Y}{\partial t}=D_g\frac{\partial^2 Y}{\partial r^2}+\frac{2D_g}{r}\frac{\partial Y}{\partial r} \tag{6}$$

$$\frac{\partial T}{\partial t}=\alpha_g\frac{\partial^2 T}{\partial r^2}+\frac{2\alpha_g}{r}\frac{\partial T}{\partial r} \tag{7}$$

These equations can be accurately solved with finite difference technique using appropriate boundary conditions and provide the solution in terms of species concentration profiles (fuel vapour and oxidiser) and temperature profile for the inflame and post flame zones respectively.

The boundary and initial conditions based on this combustion model are as follows

$$at\ r=r_f;\ T=T_f,\ Y_{o,f}=0,\ Y_{F,f}=0$$

$$at\ r=r_\infty;\ T=T_\infty,\ Y_{o,\infty}=0.232,$$

$$at\ t=0;\ r=r_{lo},\ T=T_b,\ Y_{F,S}=1.0$$

where $r_l=r_{lo}\left(1-t/t_d\right)^{1/2}$ for $\left(0\le t\le t_d\right)$, is the moving boundary condition coming out from the d^2-*law*. Here, T_f and T_∞ are temperatures at the flame and ambient atmosphere respectively.

$Y_{F,s}$ and $Y_{F,f}$ are fuel mass fractions respectively at the droplet surface and flame. $Y_{o,\infty}$ and $Y_{o,f}$ are oxidiser concentrations in the ambience and at the flame respectively, t is the instantaneous time, t_d is the combustion lifetime of the droplet, r_{lo} is the original or initial droplet radius and r_l is the instantaneous droplet radius at time "t".

The location where the maximum temperature $T=T_f$ or the corresponding concentrations $Y_{F,f}=0$ and $Y_{o,f}=0$ occur, was taken as the flame radius r_f. Instantaneous time "t" was obtained from the computer results whereas the combustion lifetime "t_d" was determined from the relationship coming out from the d^2-*law*.

Other parameters like instantaneous flame to droplet diameter ratio (F/D), flame standoff distance (F-D)/2, dimensionless flame diameter (F/D_0) etc, were then calculated as a function of time. Products species concentrations (CO, NO, CO2 and H2O) were estimated using Olikara and Borman code [34] with gas phase code of the present study.

3.2. Solution Technique

Equations (6) and (7) are a set of linear, second order, parabolic partial differential equations with variable coefficients. They become quite similar when thermal and mass diffusivities are made equal for unity Lewis number. They can be solved by any one of the following methods such as weighted residual methods, method of descritisation in one variable, variables separable method or by finite difference technique. In weighted residual methods, the solution is approximate and continuous, but these methods are not convenient in present case since one of the boundary condition is time dependent.

The method of descritisation in one variable is not suitable since it leads to solving a large system of ordinary differential equations at each step and therefore time consuming. Variables separable method provides exact and continuous solution but cannot handle complicated boundary conditions.

Keeping in view the limitations offered by other methods, "finite difference technique" is chosen (which can deal efficiently with moving boundary conditions, as is the case in present work) and successfully utilised in solving equations (6) and (7). The approach is simple, fairly accurate and numerically efficient [35]. Here the mesh size in radial direction is chosen as h and in time direction as k.

Using finite difference approximations, equations (6) and (7) can be descritised employing three point central difference expressions for second and first space derivatives, and the time derivative is approximated by a forward difference approximation resulting in a two level, explicit scheme (eqn 8), which is implemented on a computer.

$$T_m^{n+1}=\alpha\lambda_1\left(1-p_m\right)T_{m-1}^n+\left(1-2\alpha\lambda_1\right)T_m^n+\alpha\lambda_1\left(1+p_m\right)T_{m+1}^n \quad (8)$$

Here, $\lambda_1(mesh\ ratio)=k/h^2$, $p_m=h/r_m$,

$$r_m=r_{lo}+mh',\ Nh=r_\infty-r_{lo},\ m=0,1,2....N.$$

The solution scheme is stable as long as the stability condition $\lambda_1<1/2$ is satisfied. Equations (6) and (7) can also be descritised in Crank-Nicholson fashion, which results in a six point, two level implicit scheme. From a knowledge of solution at the n^{th} time step, we can calculate the solution at the $\left(n+1\right)^{th}$ time step by solving a system of $(N-1)$ tridiagonal equations. Although the resulting scheme is more accurate, the cost of computation is fairly high.

3.3. Multicomponent Droplet Vaporisation and Combustion Models

3.3.1. Droplet Vaporisation Model

Multicomponent droplet vaporisation and combustion models for the case when d^2-*law* is followed are formulated and effects of air-fuel vapour mixing and Lewis number are obtained on droplet vaporisation behaviour.

After that, a more realistic MC diffusion limit model with convection is also evolved and compared with other models.

For pure vaporisation/evaporation case, the evaporation constant k_{ev} of the multicomponent mixture is given as [17]:

$$k_{ev}=\frac{8\bar{\lambda}_g}{\bar{C}_{pg}\bar{\rho}_l}\ln\left[1+\frac{\bar{C}_{pg}\left(T_\infty-\bar{T}_{b_l}\right)}{\sum y_{ilo}L_i}\right] \quad (9)$$

where, $\bar{\lambda}_g,\bar{C}_{pg}$ are respectively the gas mixture thermal conductivity and specific heat.

$\bar{T}_{b_l}, T_\infty$ are liquid mixture boiling point temperature and ambient temperature respectively.

L_i is the latent heat of vaporisation of a particular species, and y_{ilo} is the initial liquid phase mass fraction of a species, $\bar{\rho}_l$ is the liquid mixture density.

With the assumption that surface temperature is equal to its boiling point $\left(T_s=T_b\right)$, d^2-*law* can be followed, where the instantaneous droplet radius r_l can be determined from

$$r_l=r_{lo}\left(1-t/t_{ev}\right)^{1/2} \quad (10)$$

here, r_{lo} is the initial or original droplet radius and t_{ev} is the droplet lifetime of multicomponent droplet (for pure vaporization case)

That is:

$$t_{ev} = 4r_{lo}^{\,2}/k_{ev} \tag{11}$$

Once t_{ev} is calculated, it is used as an input to the code developed for solving the species diffusion equation in the liquid phase. Other variables needed as input are liquid phase thermal diffusivity of the species, gas and liquid phase densities and diffusion coefficients, liquid phase Lewis number and initial droplet radius.

Apart from these, certain parameters related to droplet evaporation need to be determined which are discussed below.

Generally, initial liquid side mass fractions of the bicomponent fuel droplet are known or chosen, then the corresponding liquid side mole fractions can be determined using

$$x_{mls} = \frac{y_{mls}/W_m}{\sum_i (y_i/W_i)} \tag{12}$$

is the species liquid side mole fraction at the droplet surface, y_{mls} is the species liquid side mass fraction at the droplet surface, W_m is the species molecular weight.

The gas side mole fraction can be calculated by the relation

$$\frac{x_{mgs}}{x_{mls}} = \frac{1}{P}\exp\left(\frac{L_m}{R_m}\left(\frac{1}{T_{b_m}} - \frac{1}{T_s}\right)\right) \tag{13}$$

here, T_s is the surface temperature, $P = 1$atm, L_m, R_m and T_{b_m} are latent heat, specific gas constant and boiling point of the species respectively. Then y_{mgs} (species gas side mass fraction at the droplet surface) can be obtained from the relation

$$y_{mgs} = \frac{x_{mgs}W_m}{\sum_i x_i W_i} \tag{14}$$

$$\text{also, } Y_{F,S} = \sum_i y_{igs} = \sum_i y_{mgs} \tag{15}$$

and fractional vaporisation rate of the species, ε_m is given as:

$$\varepsilon_m = y_{mgs} + y_{mgs}\left(1 - Y_{F,S}\right)\Big/ Y_{F,S} \tag{16}$$

For a multicomponent droplet vaporisation model, the transfer number B_m for a particular species is given by the relation:

$$B_m = \frac{y_{mgs}}{\varepsilon_m - y_{mgs}} \tag{17}$$

y_{mgs} and B_m are used as input to the code.

The solution of the species diffusion equation gives the variation of species concentration or species mass fraction from centre of droplet to the droplet surface as a function of time. One can also calculate the species vaporisation rate (m_i) using the relation

$$m_i = 4\pi\bar{\rho}_g \bar{D}_g r_l \varepsilon_i \ln\left(1 + B_m\right) \tag{18}$$

$\bar{\rho}_g$, $\bar{D}_g$ are gas phase mixture density and diffusion coefficient respectively and r_l is the instantaneous droplet radius which can be determined as a function of time from the d^2-*law*, for a known initial droplet size.

3.3.2. Droplet Combustion Model

Another expression for mixture burning constant is derived [17] when considering combustion

$$k_b = \frac{8\bar{\lambda}_g}{\bar{C}_{pg}\bar{\rho}_l}\ln\left[1 + \frac{\bar{C}_{pg}(T_f - \bar{T}_{b_l}) + [(Y_{o,\infty}/\Sigma y_i \nu_i)](\Sigma y_i Q_i)}{\Sigma y_i L_i}\right] \tag{19}$$

T_f is the flame temperature of the bicomponent liquid fuel mixture determined from the stoichiometric combustion reaction, Q_i is the heat of combustion of a particular species. The transfer number for combustion is given for a particular species as:

$$B_m = \frac{\nu_i Y_{o,\infty} + y_{igs}}{\varepsilon_i - y_{igs}} \tag{20}$$

Here ν_i is defined as a ratio of mass of fuel to mass of oxygen, obtained from the stoichiometric combustion reaction of the particular species. The computer programme then gives variation of species liquid mass fraction with dimensionless radius at different times of droplet burning.

3.3.3. Multicomponent Diffusion Limit Vaporisation Model with Convection (Variable Surface Temperature)

An attempt has been made to develop a more realistic bicomponent droplet vaporisation model by relaxing the assumption of Ts = Tb. Once this assumption is dropped, the problem of bicomponent droplet vaporisation becomes involved, since one has to solve the energy equation (equation 21), in the liquid phase in addition to the liquid phase species mass diffusion equation (equation 43).

The solution of energy equation gives the variation of droplet surface and center temperatures as a function of dimensionless radius at different times of droplet burning or droplet vaporisation, as the case may be. The variation of droplet surface temperature with time then becomes an important input parameter for the solution of liquid phase mass diffusion equation, in addition d^2-*law* does not hold for this particular case.

Mass diffusion in the liquid phase is of primary importance in the vaporisation process for a multicomponent fuel. Therefore for studying multicomponent droplet evaporation/combustion, a detailed liquid phase analysis is a prior step.

3.4. Liquid Phase Analysis

3.4.1. Liquid Phase Energy Equation

For the development of liquid phase model, "conduction limit" approach is followed where conduction is the only mode of heat transport from the energy arriving at the droplet surface to its interior. Here, the droplet temperature is varying both spatially and temporally. The system is spherically symmetric with no internal liquid motion. Gas phase is assumed quasi-steady. Clausius-Clapeyron relation describes the phase equilibrium at the liquid-vapour interface. The liquid phase heat diffusion equation is given as:

$$\frac{\partial T_l}{\partial t} = \frac{\alpha_l}{r^2}\frac{\partial}{\partial r}\left(r^2\frac{\partial T_l}{\partial r}\right) = \alpha_l\left[\frac{\partial^2 T_l}{\partial r^2} + \frac{2}{r}\frac{\partial T_l}{\partial r}\right] \tag{21}$$

where, T_l and α_l are liquid phase temperature and thermal diffusivity respectively.

Initial and boundary conditions being

$$T(r,0) = T_0(r) \tag{22}$$

$T_0(r)$ is the initial temperature distribution

$$\left(\frac{\partial T}{\partial r}\right)_{r=0} = 0 \tag{23}$$

$$mH = mL + \left(4\pi^2\lambda_l\frac{\partial T}{\partial r}\right)_{r_s} \tag{24}$$

Where r_s is the radius at the droplet surface, λ_l is the liquid thermal conductivity.

The above equation represents the energy conservation at the interface, L and H are specific and effective latent heat of vaporisation respectively.

The complete solution of equation (21) requires certain quasi-steady gas phase relations (with respect to combustion) in terms of droplet surface temperature T_s given as:

$$\hat{Q}_1 = \left(1 - Y_{F,S}\right)\left[(\hat{T}_\infty - \hat{T}_s + \nu Y_{o,\infty}\hat{Q}_2)\right]\Big/ Y_{F,S} + \nu Y_{o,\infty} \tag{25}$$

$$\hat{m} = \ln\{1 + (\hat{T}_\infty - \hat{T}_s + \nu Y_{o,\infty}\hat{Q}_2)\big/\hat{Q}_1\} \tag{26}$$

where, $\hat{Q}_1$ is a dimensionless parameter, $\hat{m}$ is dimensionless mass evaporation rate,

$\hat{Q}_2 = Q/L$, Q is the heat of combustion of fuel, ν is stoichiometric fuel-oxygen ratio on mass basis, $Y_{F,S}$ is the fuel vapour mass fraction at the droplet surface, which can be determined from Clausius-Clapeyron relation (equation 27) and $Y_{o,\infty}$ is oxidiser mass fraction in ambient atmosphere = 0.232.

Ambient temperature T_∞, droplet surface temperature T_s and boiling point temperature T_b are non-dimensionalised by defining $\hat{T}_\infty = \frac{T_\infty C_{pg}}{L}$, $\hat{T}_s = \frac{T_s C_{pg}}{L}$ and $\hat{T}_b = \frac{T_b C_{pg}}{L}$ where C_{pg} is the gas phase specific heat. The Clausius-Clapeyron relation can be written as [36]:

$$Y_{F,S} = \{(1 + W_g/W_F(P_\infty \exp([C_{pg}/R][1/\hat{T}_s - 1/\hat{T}_b]) - 1)\}^{-1} \tag{27}$$

W_g is the average molecular weight of all gas phase species except fuel, at the surface, W_F is the molecular weight of the fuel. R is the specific gas constant of the fuel, P_∞ is equal to one atmosphere.

3.4.2. Solution Technique

A convenient method of solving problems with moving boundary is to change the moving boundary to a fixed boundary using coordinate transformation.

Equation (21) is a linear, second order partial differential equation which can be solved together with initial and boundary conditions using coordinate transformation method.

Therefore, we have

$$\hat{r} = r/r_s(t),\ \hat{t} = \alpha_l\int_0^t (r_S(t))^{-2}\,dt,\ \hat{T} = C_{pg}T/L \tag{28}$$

Where $\hat{r}$, $\hat{t}$ and $\hat{T}$ are the transformed radial coordinate, time and temperature respectively. $r_s(t)$ is the instantaneous droplet radius at the surface at time t. The transformed equations are descritised using finite difference technique employing three point central difference expressions for second space derivative and central difference expression for first space derivatives while the time derivative is approximated by a forward difference expression resulting in a two level, explicit scheme.

The heat diffusion equation (equation 21) governing liquid phase temperature variation takes the form

$$\frac{\partial\hat{T}}{\partial\hat{t}} = \frac{1}{\hat{r}^2}\frac{\partial}{\partial\hat{r}}\left(\hat{r}^2\frac{\partial\hat{T}}{\partial\hat{r}}\right) - \hat{m}K\hat{r}\left(\frac{\partial\hat{T}}{\partial\hat{r}}\right) \tag{29}$$

and the corresponding initial and boundary conditions are

$$\hat{T}(\hat{r},0) = \hat{T}_0(\hat{r}) \tag{30}$$

$$\left(\frac{\partial\hat{T}}{\partial\hat{r}}\right)_{\hat{r}=0} = 0 \tag{31}$$

$$\left(\frac{\partial\hat{T}}{\partial\hat{r}}\right)_{\hat{r}=1} = \hat{m}K'(\hat{H} - 1) \tag{32}$$

K' and K are dimensionless parameters defined as:

$K' = \lambda_g/\lambda_l$ and $K = (\lambda_g/\lambda_l)/(C_{pg}/C_{pl})$. For simplicity we have assumed gas and liquid phase specific heats and thermal conductivities as equal, hence K and K' are equal. For combustion under subcritical conditions, K is of the

order of 0.1 to 0.5. We now impose a mesh:

$$[(\hat{r}_i,\hat{t}_j):\hat{r}_i=ih,\ i=0,1,2,\ldots,N;\ \hat{t}_j=(jk),\ j=0,1,2,3,..],$$

here h is the mesh size for $\hat{r}$ and k is the time step. We then use the following finite difference approximations

$$\left(\frac{\partial\hat{T}}{\partial\hat{t}}\right)_{(\hat{r}_i,\hat{t}_j)} \cong \frac{\hat{T}_{i,j+1}-\hat{T}_{i,j}}{k} \tag{33}$$

$$\left(\frac{\partial\hat{T}}{\partial\hat{r}}\right)_{(\hat{r}_i,\hat{t}_j)} \cong \frac{\hat{T}_{i+1,j}-\hat{T}_{i-1.j}}{2h} \tag{34}$$

$$\left(\frac{\partial^2\hat{T}}{\partial\hat{r}^2}\right)_{(\hat{r}_i,\hat{t}_j)} \cong \frac{\hat{T}_{i+1,j}-2\hat{T}_{i,j}+\hat{T}_{i-1,j}}{h^2} \tag{35}$$

$$\text{Where, } \hat{T}_{i,j}=\hat{T}(\hat{r}_i,\hat{t}_j) \tag{36}$$

In general

$$\left(\frac{\partial\hat{T}}{\partial\hat{r}}\right)_{(\hat{r}_i,\hat{t}_j)} \cong \frac{1}{h}\left(C_2\hat{T}_{i+1,j}+C_1\hat{T}_{i,j}+C_0\hat{T}_{i-1,j}\right) \tag{37}$$

Special cases being
Central Difference Formula
(C_2 = 1/2 , C_1 = 0, C_0 = -1/2)
Forward Difference Formula
(C_2 = 1, C_1 = -1, C_0 = 0)
Backward Difference Formula
(C_2 = 0, C_1 =1, C_0 = -1)

Substituting in equation (29) and simplifying, we get the two level explicit scheme given by equation (38):

$$\hat{T}_{i,j+1}=\lambda_1\hat{T}_{i+1,j}\left(1+C_2hf_{i,j}\right)+\hat{T}_{i,j}\left(1-2\lambda_1+C_1h\lambda_1f_{i,j}\right)$$
$$+\lambda_1\hat{T}_{i-1,j}\left(1+C_0hf_{i,j}\right), \tag{38}$$

where λ_1 (mesh ratio) = k/h^2

$$\begin{aligned}&i=1,2,3,\ldots\ldots,N-1\\&j=0,1,2,3,\ldots\ldots\\&\text{and}\\&f_{i,j}=(2/\hat{r}_i)-\hat{m}_jK\hat{r}_i\end{aligned} \tag{39}$$

Further, initial and boundary conditions may be descritised to obtain following additional equations:

$$\hat{T}_{0,i}=(\hat{T}_0)_i \tag{40}$$

$$(\hat{T}_0)_j=(\hat{T}_1)_j \tag{41}$$

$$(\hat{T}_N)_j=(\hat{T}_{N-1})_j+hK'\hat{m}_j(\hat{H}_j-1) \tag{42}$$

Solution of heat diffusion equation (21) provides the radial variation of droplet temperature at different times of burning. Prior solution of equation (21) is necessary for determining the species concentration or mass fraction distribution within a multicomponent liquid fuel droplet.

3.4.3. Liquid Phase Mass Diffusion Equation

Spherically symmetric, multicomponent liquid phase mass diffusion with no internal circulation is written as:

$$\frac{\partial Y_{l,m}}{\partial t}=D_l\left(\frac{\partial^2Y_{l,m}}{\partial r^2}+\frac{2}{r}\frac{\partial Y_{l,m}}{\partial r}\right) \tag{43}$$

where, $Y_{l,m}$ is the concentration or mass fraction of the mth species in the liquid, and D_l is liquid mass diffusivity which in this case is much smaller than liquid phase thermal diffusivity α_l , hence liquid phase Lewis number, $Le_l >> 1$.

The boundary condition at the liquid side of the droplet surface is

$$\left.\frac{\partial Y_{l,m}}{\partial r}\right]_s=\frac{\rho_gD_g}{\rho_lD_lr_l}\ln[1+B]\left[Y_{l,ms}-\varepsilon_m\right] \tag{44}$$

m denotes particular species

r_l is the instantaneous droplet radius at time " t "

ε_m *is species* fractional mass vaporisation rate

B is the transfer number D_l and D_g are liquid and gas phase mass diffusivities respectively

ρ_l and ρ_g are respectively the liquid and gas phase densities

At the center of the droplet, symmetry yields

$$\left.\frac{\partial Y_{l,m}}{\partial r}\right]_{r=0}=0 \tag{45}$$

A uniform initial liquid phase composition for the droplet is chosen, given as:

$$Y_{l,m}(0,r)=Y_{l,mo} \tag{46}$$

Equation (43) with boundary conditions must be applied concurrently with phase equilibrium conditions and heat diffusion equation (21) to obtain the complete solution.

For a single component fuel, phase equilibrium is expressed by the Clausius-Clapeyron equation and ε_m is unity. For a multicomponent fuel, Raoult's law provides for the phase equilibrium and $\varepsilon_m \neq 1$.

3.4.4. Solution Technique

Equation (43) is a linear, second order partial differential

equation. Using coordinate transformation by defining certain dimensionless variables, we have

$$\zeta = \frac{r}{R(t)},\ \tau = \frac{\alpha_l t}{r_{lo}^{\ 2}},\ r_s(\tau) = \frac{R(t)}{r_{lo}},\ \beta = \frac{1}{2}\frac{d}{d\tau}(r_s^{\ 2}),\ \overline{Y} = \frac{(Y_{lm} - Y_{lm0})}{Y_{lm0}} \quad (47)$$

here, r is spherical radial coordinate, r_{lo} is original or initial droplet radius, t is instantaneous time, $R(t)$ is instantaneous droplet radius at time t, ζ is dimensionless radial coordinate, τ is non-dimensional time, $r_s(\tau)$ is instantaneous non-dimensional droplet radius, $\overline{Y}$ is dimensionless mass fraction.

After transformation, liquid phase mass diffusion equation (equation 43) for the mth species can be written as:

$$\frac{1}{\gamma}\left(r_s^{\ 2}\frac{\partial \overline{Y}}{\partial \tau} - \beta\zeta\frac{\partial \overline{Y}}{\partial \zeta}\right) = \frac{\chi_d}{\zeta^2}\frac{\partial}{\partial \zeta}\left(\zeta^2\frac{\partial \overline{Y}}{\partial \zeta}\right) \quad (48)$$

where, γ is taken as reciprocal of Lewis number "Le_l", and χ_d is a dimensionless parameter defined as a ratio of effective mass diffusivity to mass diffusivity (equal to unity for the present case).

Boundary condition at the liquid side of the droplet surface (equation 44) becomes

$$\left.\frac{\partial \overline{Y}}{\partial \zeta}\right]_{\zeta=1} = \frac{\rho_g D_g}{\rho_l D_l}\ln[1+B]\left[\overline{Y}_s - \varepsilon_m\right] \quad (49)$$

Boundary condition at the droplet center (equation 45) is written as:

$$\left.\frac{\partial \overline{Y}}{\partial \zeta}\right]_{\zeta=0} = 0 \quad (50)$$

Equation (46) representing initially chosen composition takes the form

$$\overline{Y}(0,\zeta) = \overline{Y}_0 \quad (51)$$

Equation (48) can be rewritten as:

$$r_s^{\ 2}\frac{\partial \overline{Y}}{\partial \tau} - \beta\zeta\frac{\partial \overline{Y}}{\partial \zeta} = \gamma\chi_d\left(\frac{\partial^2 \overline{Y}}{\partial \zeta^2} + \frac{2}{\zeta}\frac{\partial \overline{Y}}{\partial \zeta}\right) \quad (52)$$

Equation (52), along with equations (49) to (51) are then descritised using forward difference formula for first derivatives with respect to τ and ζ and central difference formula for the second derivative with respect to ζ. After simplification, final descritised form of equation (52) is obtained as a two level explicit scheme:

$$\overline{Y}_j^{n+1} = \frac{\lambda_1 \overline{Y}_{j+1}^n}{(1-k\tau_n)}\left[\beta\zeta_j(\Delta\zeta) + \gamma\chi_d + \frac{2\gamma\chi_d(\Delta\zeta)}{\zeta_j}\right] - \frac{\lambda_1 \overline{Y}_j^n}{(1-k\tau_n)}\left[\beta\zeta_j(\Delta\zeta) + 2\gamma\chi_d + \frac{2\gamma\chi_d(\Delta\zeta)}{\zeta_j}\right] + \overline{Y}_j^n + \frac{\gamma\chi_d\lambda_1 \overline{Y}_{j-1}^n}{(1-k\tau_n)} \quad (53)$$

where; $\overline{Y}_j^n = \overline{Y}(\tau_n, \zeta_j)$, $\lambda_1 = \frac{\Delta\tau}{(\Delta\zeta^2)}$ is the mesh ratio kept < ½ for a stable solution, k is time step, $\Delta\tau$ is dimensionless time step, $\Delta\zeta$ is mesh size in ζ direction, τ_n is non-dimensional time = n $\Delta\tau$ and $\zeta_j = j\Delta\zeta$, $j = 1,2,....,M-1$

Equations (49) to (51) after descritisation take the form

$$\overline{Y}_M^n - \overline{Y}_{M-1}^n = \Delta\zeta\frac{\rho_g D_g}{\rho_l D_l}\ln[1+B][\overline{Y}_s - \varepsilon_m] \quad (54)$$

$$\overline{Y}_1^n - \overline{Y}_0^n = 0,\ \text{for } n = 0,1,2, \quad (55)$$

$$\overline{Y}_j^0 = \overline{Y}(0),\ \text{for } j = 0,1,2,\ \ ,\ \text{M} \quad (56)$$

The solution of equation (43) gives the variation of species mass fraction within the multicomponent liquid droplet as a function of droplet radius at different times of droplet burning.

Once tested for a pure component (n-octane) fuel droplet undergoing spherically symmetric combustion, a heptane-dodecane bicomponent droplet vaporisation model ($D_0 = 280\mu m$) with variable surface temperature was developed for the case where $Re_g = 100$ (convective situation). The gas phase processes were considered to be quasi-steady. The bicomponent liquid fuel droplet contained an initial liquid mass fraction of (50-50)% heptane-dodecane mixture with conditions of ambient pressure P_∞ = 1 atmosphere, ambient temperature T_∞=1000 K, Le_l = 10 and gas phase Prandtl number $Pr_g = 1$ (since quasi-steady gas phase).

Further, equations (25) and (26) for $\hat{Q}_1$ and $\hat{m}$ were modified as equations (57) and (58) respectively for pure vaporisation case of a bicomponent fuel droplet made up of (n-heptane + n-dodecane) mixture at the given conditions of ambient pressure and temperature of one atmosphere and 1000 K respectively

$$\hat{Q}_1 = \left(1 - Y_{F,S_{mix}}\right)\left[\hat{T}_\infty - \hat{T}_s\right] \Big/ Y_{F,S_{mix}} \quad (57)$$

$$\text{and } \hat{m} = \ln\left\{1 + \left[\hat{T}_\infty - \hat{T}_s\right] \Big/ \hat{Q}_1\right\} \quad (58)$$

After determining $\hat{Q}_1$ and $\hat{m}$, plots of $\hat{Q}_1$ and $\hat{m}$ with $\hat{T}_s$ were obtained. The next step involved the calculation of vaporisation/evaporation lifetime t_{ev} of the bicomponent droplet vaporising in a convective environment using the relation:

$$t_{ev} = \frac{\rho_l D_0^{\,2}}{8\bar{\lambda}_g / \bar{C}_{pg} \ln(1+B)\left(1+0.3Re_g^{0.5}Pr_g^{0.33}\right)} \qquad (59)$$

For this particular case where $T_s \neq T_b$, the bicomponent droplet transfer number (or B number), fractional vaporisation rate (ε), mass fraction of the fuel mixture at the droplet surface $Y_{F,S}$ and dimensionless parameter β will not be constant but will vary with droplet surface temperature and time. The plots of B, ε, $Y_{F,S}$ and β against dimensionless time τ_n were then obtained by curve fitting and the curve fit equations were incorporated in the computer code for solving the multicomponent liquid phase mass diffusion equation (equation 43).

4. Results and Discussion

Three different categories of fuels namely, alkanes, alcohols and biodiesels were selected to isolate the effects of various thermophysical properties on important combustion and emission characteristics. It was observed that dimensionless flame diameter F/D_0 is influenced primarily by the fuel boiling point. The same conclusion could be drawn for the variation of F/D ratio and flame standoff distance with time. Also, the F/D ratio was found to increase throughout the droplet burning period, suggesting transient burning. From $(D/D_0)^2$ versus time plot, it was observed that for steady state burning, droplet lifetime was highest for the fuel having smallest burning constant (from the relationship coming out from the *d^2-law* and burning rate variation was low for ethanol in comparison with methyl linoleate and n-heptane.

Important species concentrations in terms of NO, CO, CO_2 and H_2O were quantified for pure fuels and their blends. Multicomponent droplet combustion model was evolved and compared with model of Shaw [22] for the same fuel and burning conditions suggesting that present model was accurate and simpler. For a hexane-decane droplet vaporising at 1 atm and 1000 K, substantial effect of mixing of air and fuel vapours was observed on the vaporisation behaviour and should be accounted for in MC droplet modelling. Practical liquids have high Lewis number (of the order of 30). Profound effect on vaporisation characteristics was noted when Lewis number was varied.

In addition, a more detailed multicomponent vaporisation model was developed and compared with various models available in literature. It was felt that the present model could prove out to be more effective for application in spray analysis due to its simplicity.

4.1. Effect of Pure Fuels on Dimensionless Flame Diameter, F/D Ratio, Flame Standoff Distance, Square of Dimensionless Droplet Diameter and Mass Burning Rate

A plot of dimensionless flame diameter with dimensionless time for a 2000 μm droplet of different fuels burning under standard conditions is shown in Fig 1. Three different categories of fuels namely alkanes, alcohols and biodiesels were chosen to isolate the effect of their thermophysical and transport properties on combustion characteristics. It was observed that F/D_0 increased with an increase in the boiling point of the fuel. As a result, F/D_0 values were highest for biodiesels, followed by alkanes and alcohols. For each fuel checked, F/D_0 maximised in the 20–25 % lifetime range.

In Figure 2, F/D ratio also known as flame standoff ratio was plotted against dimensionless time for different fuels such as methyl linoleate, n-heptane and ethanol for a droplet diameter of 100 microns. This ratio is important in droplet combustion since it shows whether the burning is quasi-steady (where this ratio assumes a large constant value) or non steady as evident from experimental observations where the ratio increases throughout the droplet burning period. The F/D ratio for the present work increases throughout the droplet burning period suggesting transient droplet burning irrespective of the type of fuel.

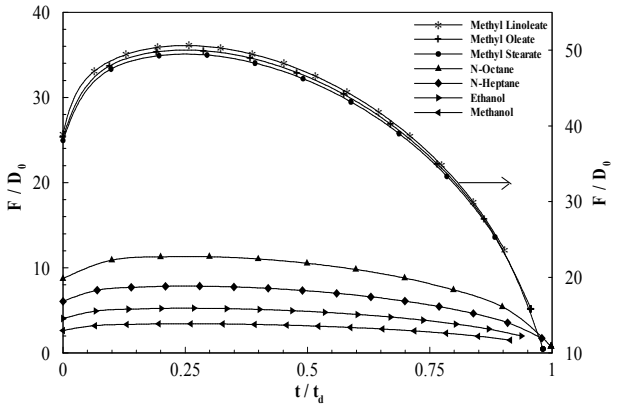

Figure 1. *Effect of fuel properties on the variation of dimensionless flame diameter F/D0 with dimensionless time t/td*

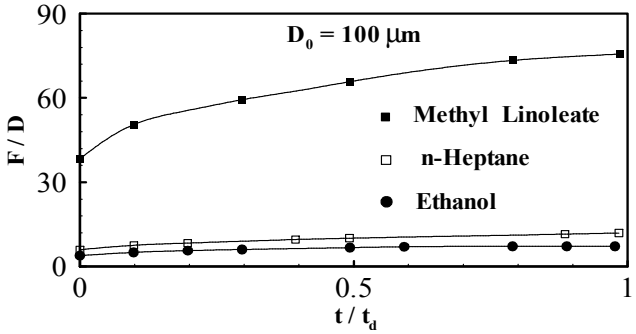

Figure 2. *Effect of fuels on F/D ratio behavior with dimensionless time.*

This is consistent with experimental observations. It is further noted that F/D values increase with an increase in the boiling point, being highest for biodiesel fuel (methyl linoleate), followed by alkane (n-heptane) and alcohol (ethanol).

When flame standoff distance was plotted against dimensionless time for n-heptane, ethanol and methyl linoleate (Fig 3), it was observed that flame standoff distance increased with an increase in boiling point of fuel.

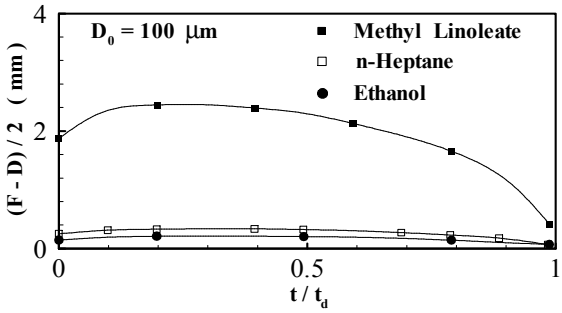

Figure 3. *Flame standoff distance versus time*

Variation of dimensionless droplet diameter squared $(D/D_0)^2$ with time was obtained for n-heptane, ethanol and methyl linoleate as shown in Fig 4. The trend showed a linear variation of $(D/D_0)^2$ with t/t_d . It was noted that droplet lifetime was highest for ethanol followed by methyl linoleate and n-heptane which could be justified from the inverse relationship between lifetime and burning constant coming out from the d^2-*law* i.e $t_{d_{SS}} = 4r_{lo}^{\ 2} / k_{b_{ss}}$.

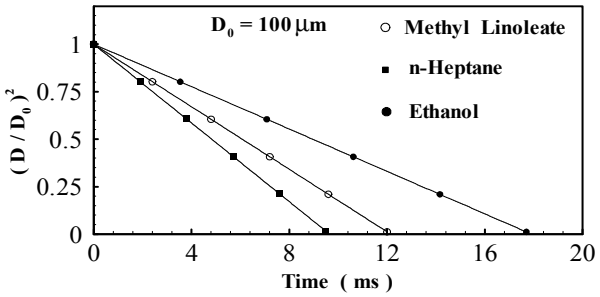

Figure 4. *Dimensionless droplet diameter squared against time*

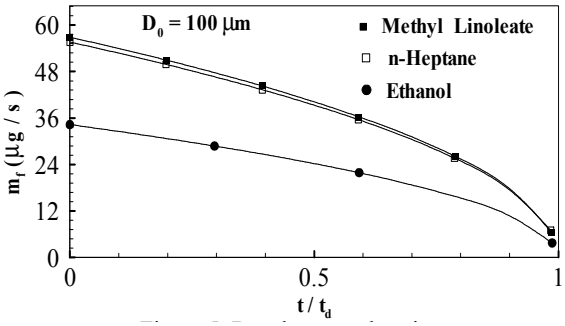

Figure 5. *Droplet mass burning rate*

Mass burning rate variation with dimensionless time t/t_d for methyl linoleate, n-heptane and methanol droplets is shown in Fig 5. Results suggest that for a 100 micron droplet, m_f values are highest at the start of combustion for methyl linoleate followed by n-heptane and ethanol. The values for different fuels were calculated using equation 60, given below, which is a function of liquid density and burning constant

$$m_f = \pi r_l \rho_l k_b / 2 \tag{60}$$

Effect of fuels on emission characteristics of a spherical combusting droplet

Most experiments related to droplet burning have been concerned primarily with combustion aspects such as measurement of droplet and flame temperatures, flame movement, droplet lifetimes, burning rates etc. As a result, relatively less experimental data related to emission characteristics is available in literature. Such information is needed to examine the formation and destruction of pollutants such as soot, unburned hydrocarbons, NO_X, CO and CO_2 and subsequently to establish design criteria for efficient and stable combustors.

For the determination of species concentration profiles around the burning spherical droplet, the following procedure was adopted.

Adiabatic flame temperature determined earlier, using first law of thermodynamics together with other input data was used to solve numerically, the gas phase energy equation (7) with the help of a computer programme. The solution obtained was in the form of temperature profile at each time step starting from the droplet surface, reaching the maxima at the flame and then reducing to the ambient temperature value. The radius at which the maximum temperature occured was taken as the flame radius.

Temperature values in the vicinity of the flame were then chosen from the computed results, which were designated as number of steps (NOS). The solution of species diffusion equation (6) in the gas phase, gave the species profile (fuel and oxidiser). It was observed that the fuel vapour concentration was maximum at the droplet surface and decreased gradually to the minimum value a the flame front, whereas, oxygen diffusing from the ambient atmosphere became minimum at the flame. Now for the same time step, which was used in the solution of energy equation, values or NOS of fuel mass fraction Y_F corresponding to the temperature values were taken from the computed results of the species diffusion equation.

Then for a particular fuel, $FARS$ (fuel to air ratio stoichiometric) on mass basis was calculated for the stoichiometric reaction of fuel and air at atmospheric conditions of temperature $T_\infty = 298K$, pressure $P_\infty = 1\ atmosphere$ and ambient oxidiser concentration $Y_{o,\infty} = 0.232$.

Fuel to air ratio actual ($FARA$) on mass basis was calculated next for each step where, $FARA = Y_F / 1 - Y_F$, and finally equivalence ratio, $\phi = FARA / FARS$. The values of flame temperature, equivalence ratio and ambient pressure were then used as input data for the Olikara and Borman Code [34], (modified for single droplet burning case) to obtain concentrations of important combustion products species.

Moreover, since most of the practical combustion systems operate with air as an oxidiser therefore formation of NO is a significant parameter which was another reason for our preference for the Olikara and Borman programme [34].

The behaviour of species concentrations as a function of dimensionless flame radius r/r_f across the flame zone with

finite thickness is shown in Figs 6-.9. The general mechanism of formation of products involves the conversion of the reactants to CO and H_2 on the fuel rich side. The CO and H_2 further diffuse towards the thin reaction zone, which is the flame sheet and react with increasing amount of O_2 and and get oxidised to form CO_2 and H_2O. The instantaneous temperature at the given point may affect the mechanism and the rate of these reactions. It is observed that NO concentration is maximum at the flame zone and is found to be very temperature sensitive. Results of the present study show higher than expected concentrations. However, the present work aims at providing a qualitative trend rather than quantitative using a simplified approach.

To isolate the effect of fuels on emission data, three pure fuels: n-heptane, ethanol and methyl linoleate (ml), three practical multicomponent fuels: diesel oil (DF2), gasoline and aviation gas turbine fuel (JP5) and two fuel blends: gasohol (70% gasoline+30% ethanol) and diesohol (80%dieseloil+20%ethanol) were considered for a droplet size of 100 micron burning at 1 atmosphere and 298 K, (Table 4).

Among pure fuels, (Figs 6-.9), minimum concentration of CO was 0.268 % in the flame zone contributed by ethanol (CO was minimum where CO_2 was maximum (9.635 %) at dimensionless flame radius $r / r_f = 0.9$), 1.475 % was for ml and 3.522 % for n-heptane. Minimum concentration of CO_2 was contributed by ethanol and then by n-heptane and ml in the increasing order. NO concentration was lowest for ethanol followed by n-heptane and ml in increasing manner, whereas H_2O concentration was maximum for ethanol followed by n-heptane and ml in decreasing order.

For practical fuels, DF2 accounted for lowest CO emission followed in the increasing order by JP5 and gasoline, further, DF2 contributed maximum CO_2 followed by JP5 and gasoline (lowest). NO concentrations in the increasing order were contributed by DF2, JP5 and gasoline respectively.

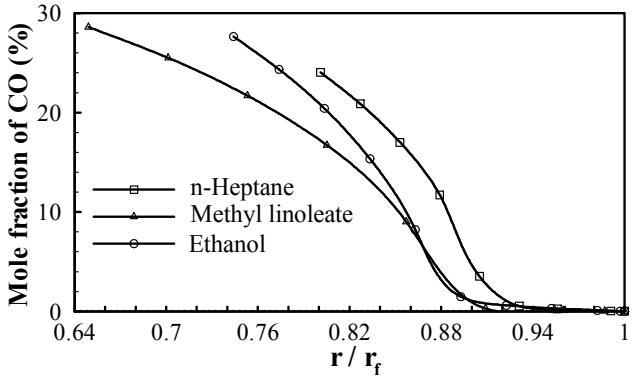

Figure 6. *Variation of CO concentration with dimensionless flame radius for a 100 micron fuel droplet burning in standard atmosphere*

It was also observed that gasohol blend gave 83.9 % less emissions with regards CO, 42 % less emissions with regards NO and 23.16 % more emissions regarding CO_2 when compared with gasoline. Whereas diesohol blend contributed 39.56% less emissions with respect to CO, 31.94 % less emissions wrt NO and 21.96 % more emissions wrt CO_2 when compared with diesel oil (DF2).

From the results, it was generally observed that fuels having higher percentage of fuel carbon and fuel hydrogen led to more CO_2 and H_2O. However, higher flame temperature might lead to dissociation thus slightly reducing CO_2 and H_2O concentrations as seen for methyl linoleate.

NO concentrations were a strong function of flame temperature, and as a result they were lowest for ethanol among pure fuels, lowest for DF2 among practical fuels and minimum for gasohol in case of blended fuels. The variation of CO, CO_2, and NO with respect to different fuels for the present work, showed similar trend when compared with experimental data obtained from engine analysis [29].

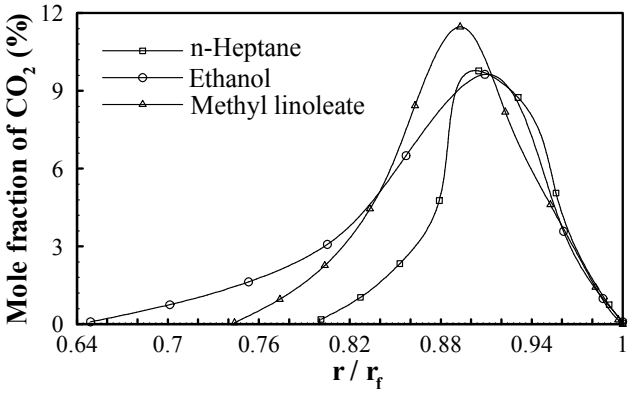

Figure 7. *CO_2 concentration*

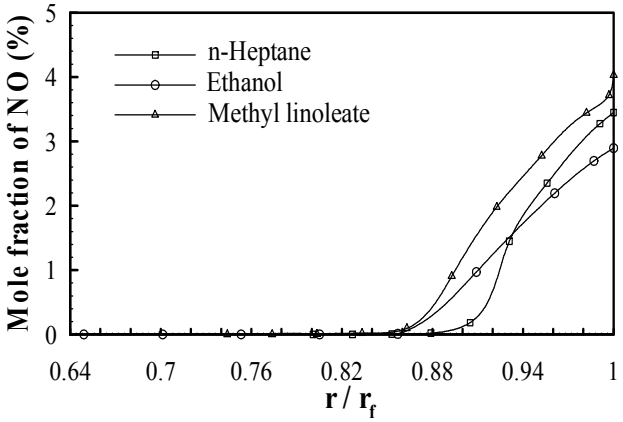

Figure 8. *NO concentration*

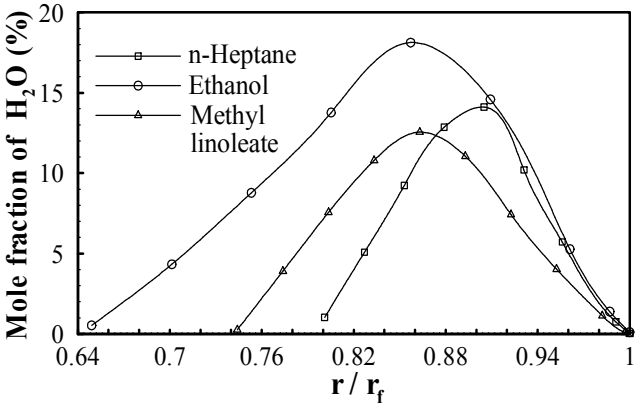

Figure 9. *H_2O concentration*

4.2. Vaporisation and Combustion Behaviour of Multicomponent Fuel Droplets

Various multicomponent droplet vaporisation and combustion models exist in literature. Some of these models seem to be oversimplified, while some are too complex to be incorporated in a spray model. The objective of the present study was to develop multicomponent droplet vaporisation and combustion models which are simple and accurate to be feasibly incorporated in spray analysis.

Law and Law [17] have shown that for the case where liquid phase species diffusion rates are slow relative to droplet surface regression rates, in other words when droplet surface temperature is equal to its boiling point temperature (Ts=Tb) and the droplet is vaporising vigorously following d^2-*law* after an initial transient period, then a similar expression for burning constant can be developed analogous to the single component case.

This analysis comprehensively reduces the complexity of the problem. A conclusion of this work is that the fractional vaporisation rate of any species ε_m at the droplet surface is equal to the initial liquid phase mass fraction of that species prior to vaporisation/combustion.

4.3. Calculation Procedure

The burning conditions for heptane-dodecane droplet were ambient pressure $P_\infty = 1 atm$, ambient temperature $T_\infty = 300K$, ambient oxidiser mass fraction $Y_{o,\infty} = 0.232$. The combustion reaction was assumed stoichiometric, with no dissociation effects. Initially assumed liquid phase mass fraction y_{ilo} was 0.4 for n-heptane. Then using equation 12, the corresponding liquid side mole fractions were determined for n-heptane and n-dodecane. The adiabatic flame temperature T_f for the mixture was determined as a next step using a computer code (developed in the present study) as 2475.47K. Following properties, $\bar{C}_{pg}$, $\bar{\rho}_l$, $\bar{\lambda}_g$, $\bar{T}_{b_l}$, $\sum_i (y_i \nu_i)$, $\sum_i (y_i L_i)$ and $\sum_i (Q_i y_i)$;(where a bar above symbols indicates mixture values) were then evaluated at a proper reference temperature and composition using relations provided elsewhere [37]. The mixture burning constant k_b was calculated from equation 19 as $5.67\times10^{-7} m^2/s$ (0.567 mm^2/s).

The gas side mole fraction for n-heptane x_{mgs} was calculated using equation 13 and the gas side mass fraction y_{mgs} was calculated using equation 14. Similarly x_{mgs}, y_{mgs} for n-dodecane were evaluated and $Y_{F,S}$ was determined using equation 15. Fractional vaporisation rate ε_m for n-heptane was obtained from equation 16 and finally the transfer number B_m (combustion) for n-heptane was determined using equation 20. Other properties such as liquid phase thermal diffusivity α_l, ρ_l, ρ_g, D_l and D_g for n-heptane were evaluated and used as input parameters to the computer code. The results are depicted in Figs 10-11.

4.4. Plots of Heptane Mass Fraction Versus Dimensionless Radius and Time

The solution of equation 43 was obtained as a variation of n-heptane mass fraction with dimensionless radius r/R at each instant of time. Here r is the radial coordinate and R or r_l is the instantaneous droplet radius. The variation of n-heptane mass fraction as a function of dimensionless radius is depicted in Fig 10 for the present study and compared with the work of Shaw [22] for the same conditions. For both models, droplet was assumed to be at its boiling point. Both results showed the same trend. From an initial chosen value of n-heptane liquid phase mass fraction $y_{ilo} = 0.4$, the mass fraction of n-heptane remained nearly constant from the center of the droplet till the value of dimensionless radius r/R was about 0.76, then as the droplet surface was approached, n-heptane began to vaporise and its mass fraction or concentration decreased abruptly.

For the present work the minimum n-heptane concentration at the surface was about 0.155 whereas for Shaw [22] it was about 0.05. The reason for the concentration of n-heptane remaining nearly constant from the center of the droplet till dimensionless radius was about 0.76 can be attributed to the fact that liquid phase mass diffusion is very small as compared to liquid phase thermal diffusion. Hence higher the value of liquid phase Lewis number Le_l, higher will be the diffusional resistance offered by the liquid and smaller will be the vaporisation. Appropriate relations for determining thermophysical and transport properties were employed for the present work. For the given conditions, $Le_l = 10$ for the present model, whereas for Shaw [22], $Le_l = 7.8$, this difference in the values of Lewis number might be the factor responsible for the higher n-heptane fraction left at the surface for the present work.

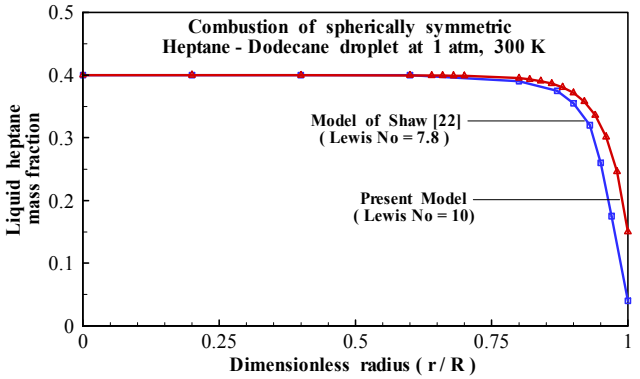

Figure 10. *Variation of liquid heptane mass fraction with dimensionless radius at a particular time*

Figure 11 shows the variation of n-heptane liquid surface mass fraction with dimensionless time for the present model, other conditions remaing same. The plot shows the liquid surface mass fraction of n-heptane varying from the initial

chosen value of $y_{ilo} = 0.4$ to a value of about 0.155. The surface mass fraction of heptane initially decreases steadily with time suggesting preferential vaporisation of the more volatile species (which is n-heptane) in the earlier stages of droplet burning and hence high vaporisation rates resembling batch distillation type behaviour.

Then the rate of decrease becomes small and continues till the end of droplet lifetime, which may be because the bicomponent droplet is assumed to be at its boiling point ($426.895K$) throughout its burning period. This high boiling point temperature will lead to the vaporisation of less volatile (higher boiling point) component from the surface and hence less droplet vaporisation rate towards the end of droplet lifetime. Authors like Tong and Sirignano [12] and Aggarwal and Mongia [18] have also suggested the same explanation.

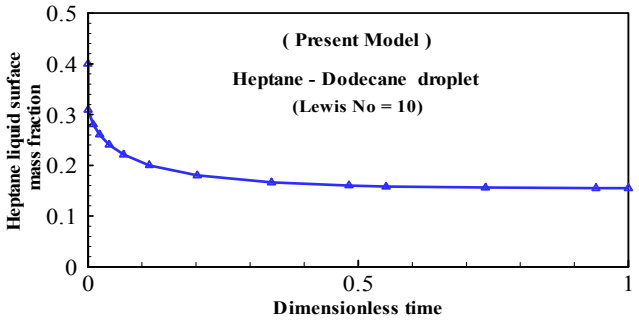

Figure 11. *Heptane liquid surface mass fraction variation with dimensionless time.*

4.5. Effect of Mixing of Air and Fuel Vapours on Vaporisation

A comparison of the variation of hexane liquid surface mass fraction with dimensionless time is made for two situations where mixing of air and fuel vapours is taken into account and the later case where mixing is not considered (Fig 12). The droplet was assumed to be vaporising at its boiling point in ambient conditions of 1 atm and 1000 *K*. Thermodynamic properties for hexane-decane mixture were calculated as a function of temperature and composition using appropriate relations [37].

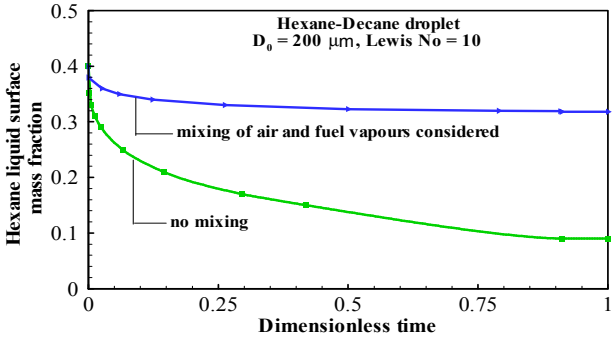

Figure 12. *Vaporisation of hexane-decane droplet (effect of mixing)*

It is observed that when mixing was neglected, a small amount of hexane fraction (about 0.09) was left at the surface at the end of droplet lifetime compared to approx 0.32 when mixing was considered. Further, the decrease in heptane mass fraction was gradual for the non-mixing case, while for the mixing case, apart from initial small decrease, the hexane mass fraction was nearly constant from dimensionless time value of about 0.5 onwards. This difference in vaporisation behaviour for the two cases could be attributed to the use of appropriate mixing rules accounting for air and fuel vapour mixing. The present result could be appreciated if experimental data was available for the same vaporising conditions, fuel and droplet size.

4.6. Effect of Lewis Number

Another important result (Fig 13) compares the effect of Lewis number on the variation of hexane liquid surface mass fraction with dimensionless time for a hexane-decane droplet, other conditions remaining same.

It was observed that the mass fraction of hexane at the droplet surface reduces gradually from an initial chosen value of 0.4 to about 0.09 at the end of lifetime, when $Le_l = 10$. Whereas for $Le_l = 30$, hexane mass fraction drops initially from 0.4 to 0.18 at dimensionless time equal to 0.16, after that becoming more or less constant till the end of droplet lifetime, where it is 0.175. The reason for more amount of hexane left at the droplet surface might be due to the high diffusional resistance offered to hexane (due to high Lewis number), discouraging it to come to the surface rapidly and hence its slow evaporation from the droplet surface. The trend in the result of the present study is in conformity with the results of other authors [19].

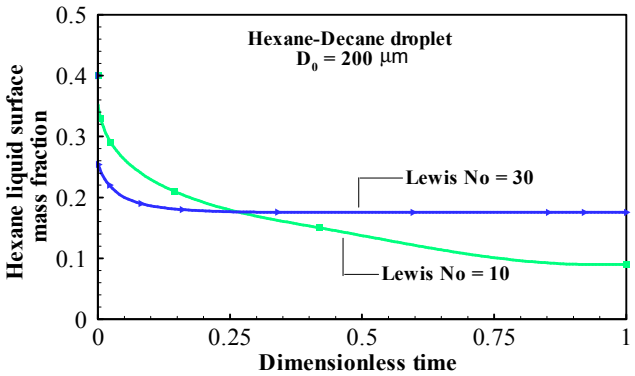

Figure 13. *Effect of Lewis number.*

4.7. Comparison between Different Vaporisation Models

As next part of the present work, different multicomponent droplet models (Figs 14-15) were compared for a heptane-dodecane droplet vaporising at 1 atmosphere and $1000\,K$. For all models, the initial liquid surface mass fraction was taken as 0.5. The present diffusion limit model (with convection) was evolved by solving transient-diffusive equations of species and energy within the liquid droplet and compared with the spherically symmetric d^2-*law* model of Law and Law [17] in Fig 14 and model of Tong and Sirignano and infinite diffusivity model in Fig 15. For the present model and that of Tong and Sirignano, Re_g = 100. The

relevant properties of heptane-dodecane mixture for the present work were evaluated as function of temperature and composition using relations provided elsewhere [37].

It was observed that for model of Law and Law, there was a steady decrease of heptane surface mass fraction due to preferential vaporisation of the more volatile species. Eventually, later in the droplet lifetime, the droplet is completely depleted of the heptane component. Another reason for the steadily decreasing heptane mass fraction may be the lower value of Le_l chosen. Because of this lower value of 10, there is a smaller resistance offered to heptane, hence its faster evaporation from the liquid surface. The droplet lifetime is about 221 ms.

For the present model, droplet lifetime is evaluated as 65 ms. It is observed that there is a sudden initial decrease in the heptane liquid surface concentration and heptane is depleted completely from the droplet when the droplet lifetime is about 10%. The trend of the present model is quite similar when compared with the model of Tong and Sirignano [12] which is also known as vortex diffusion limit model. For both, the decrease in the liquid surface concentration of heptane is sudden, occurring earlier in the lifetime but the result of Tong and Sirignano indicates that all of the heptane is not depleted from the droplet, rather it levels off at a constant value of about 0.03.

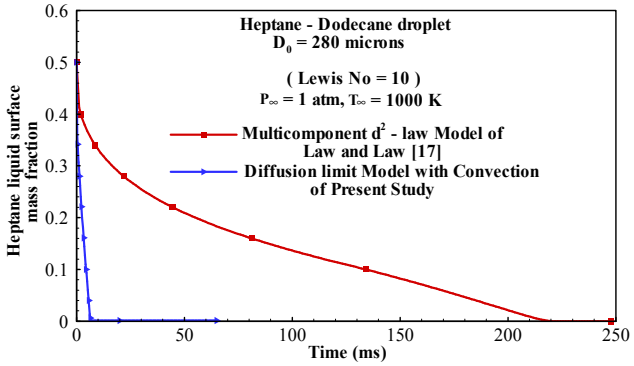

Figure 14. *Vaporisation behavior of a heptane-hexane-decane droplet (comparison between models)*

It is important to note that both the d^2-*law* model as well as infinite diffusivity model are quite approximate when compared to the present model and that of Tong and Sirignano. However, the present model offers less complexity, is quite accurate and can serve successfully in MC spray calculations.

The sudden decrease in heptane surface mass fraction earlier in the lifetime for both the studies may be due to the initially high fractional vaporisation rate of heptane which later becomes smaller as the droplet surface temperature increases but at the same time convection becomes more important leading to more efficient vaporisation which could have reduced the diffusional resistance. The difference in the results may be due to the value of Lewis number, which the authors [12] have not mentioned. The droplet lifetime for [12] is also a little higher (about 88 ms). This may be due to the bigger droplet size (360 μm).

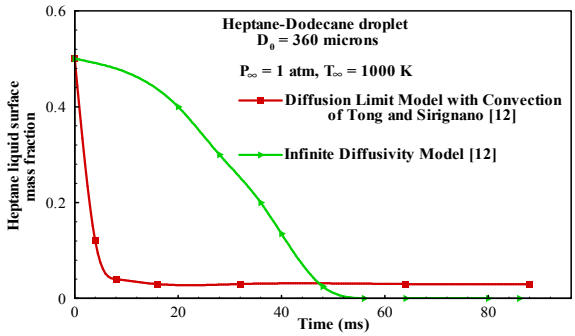

Figure 15. *Comparison of multicomponentdroplet vaporisation models*

5. Conclusions

A comprehensive, single component, diffusion controlled droplet combustion model was developed by solving numerically the time dependent energy and species conservation equations in the gas phase. It was observed that first the flame moves away from the droplet surface and then towards it, further, the flame to droplet diameter ratio was found to increase throughout the droplet burning period. These results are in conformity with the experimental observations and do not agree with the quasi-steady theory where the flame to droplet diameter ratio takes a large constant value.

The present droplet combustion model was further used to obtain the effect of fuels on important combustion parameters like dimensionless flame diameter, square of dimensionless droplet diameter and mass burning rate and a qualitative trend of emission characteristics such as CO_2, CO, NO and H_2O. It was noted that dimensionless flame diameter was influenced primarily by the fuel's boiling point. The droplet mass burning rate was the lowest for ethanol as compared to methyl linoleate (biodiesel) and n-heptane. Whereas, gasohol and diesohol proved out to be better blends than gasoline and diesel oil respectively with respect to NO and CO emissions.

In case of multicomponent droplet combustion, it was observed that for spherically symmetric combustion of a heptane-dodecane droplet, mass fraction of heptane remained nearly constant from droplet center till the value of dimensionless radius was approximately 0.76, then as droplet surface was approached, heptane began to vaporise and its mass fraction decreased rapidly to a lower value at a particular time of droplet burning.

For a 200 μm hexane-decane droplet (at its boiling point), vaporising in conditions of 1 atm and 1000 K with $Le_l = 10$, it was observed that when mixing of air and fuel vapour was ignored, a small amount of hexane mass fraction was left at the droplet surface at the end of droplet lifetime, whereas when mixing was considered, a higher concentration of hexane was present at the surface thereby altering the vaporisation behaviour. Also, an increase in Lewis number resulted in a higher mass fraction of hexane being present at the droplet surface.

A detailed multicomponent (MC) droplet vaporisation model (diffusion limit model with convection and no internal liquid circulation) was evolved by solving numerically (using finite difference technique) transient-diffusive equations of species and energy with appropriate boundary conditions for a 280 μm (heptane-dodecane) droplet vaporising at 1 atm and 1000 K with Re_g=100, and $Le_l = 10$. Roult's law was used for expressing phase equilibrium.Thermodynamic and transport properties were evaluated as a function of temperature and composition.

It was noted that there was a sudden initial decrease in the heptane liquid surface concentration from the initial assumed value of 0.5 and was completely depleted from the droplet surface very early in its lifetime. However, a 280 μm spherically symmetric heptane-dodecane droplet vaporising at its boiling point showed a steady decrease in heptane liquid surface mass fraction till the end of lifetime when it was vaporised completely. The present MC model was compared with other existing models and was found to be simpler but quite robust.

The predictions of the present work agreed well when compared with the experimental and theoretical results of other authors who have used more complicated models. The submodels developed in the present work were found to be accurate and yet simpler (requiring less CPU time) for their incorporation in spray codes where CPU economy plays a vital role.

Table 1. *Thermophysical Properties of Fuels at 298 K*

Fuel	Chemical formula	Molecular weight $kg/kmol$	Liquiddensity kg/m^3	Latent heat kJ/kg	Liquid sp.ht kJ/kgK	Boilingpoint K	Heat of comb kJ/kg	Enthalpy of formation kJ/mol
n-Heptane	C_7H_{16}	100.205	684	316.54	2.245	371.6	44557	-187.82
n-Octane	C_8H_{18}	114.232	703	301.92	2.23	399	44425	-250.105
n-Decane	$C_{10}H_{22}$	142.284	730	272	2.21	447.1	44239	-249.65
n-Hexane	C_6H_{14}	86.177	659	335	2.27	342	44733	-167.19
n-Dodecane	$C_{12}H_{26}$	170.34	749	256.36	2.21	489.5	44109	-292.16
Methanol	CH_4O	32.042	787	1101	2.55	337.8	19910	-239.22
Ethanol	C_2H_6O	46.069	783	841.56	2.46	351.5	26811	-273.77
Methyl Linoleate	$C_{19}H_{34}O_2$	294.476	880	242.43	2.08	700.66	37830	-446.94

Table 2. *Comparison of Properties with Reported Values*

Fuel	Methyl Linoleate		Methyl Oleate		Methyl Stearate	
Property	Calculated*	Reported**	Calculated*	Reported**	Calculated*	Reported**
Critical Pressure (bar) P_c	11.91	11.91	11.68	11.68	11.46	11.46
Critical Temperature (K) T_c	871.80	795.3	864.57	772.3	857.41	774.2
Critical Volume(cm^3/mol) V_c	1085.5	1085.5	1105.5	1105.5	1125.5	1125.5

*Present study, **Yuan et al. {31]

Table 3. *Computed Values of Burning Parameters*

(T_∞=298 K ,P_∞=1atmosphere,$Y_{o,\infty}$=0.232) Fuel	$(A/F)_{stoich}$	B_T	k_b $(mm^2/\sec)$	α_g $(cm^2/\sec)$
n-Heptane	15.1008	8.765	1.036	1.403
n-Octane	15.053	8.947	0.832	1.23
n-Dodecane	14.94	9.66	1.0	1.66
Methanol	6.435	2.72	0.392	1.087
Ethanol	8.953	3.384	0.5582	1.096
Methyl Linoleate	11.16	9.78	0.823	1.973

Table 4. *Variation of CO, CO_2, H_2O and NO Concentrations for Different Fuels*

Fuels	Chemical formula	Adiabatic flame temperature(K)	NO conc(%)	CO conc(%)	CO_2 conc(%)	H_2O conc (%)
n-Heptane	C_7H_{16}	2396.17	3.446	3.522	9.768	14.112
Ethanol	C_2H_6O	2289.14	2.895	0.268	9.635	18.124
Methyl linoleate	$C_{19}H_{34}O_2$	2454.0	4.028	1.475	11.47	12.55
Gasoline	C_7H_{17}	2721.63	5.866	4.66	7.666	13.021
Diesel oil (DF2)	$C_{14}H_{30}$	2626.14	5.175	1.979	8.394	13.142
ATF (JP5)	$C_{12}H_{24}$	2707.31	5.758	2.704	7.979	12.406
Gasohol	70% gasoline + 30% ethanol	2387.25	3.399	0.75	9.977	14.527
Diesohol	80 % DF2 +20 % ethanol	2409.0	3.522	1.196	10.757	13.586

References

[1] S. Okajima and S. Kumagai, "Further Investigation of Combustion of Free Droplets in a Freely Falling Chamber Including Moving Droplets", Proceedings of the Fifteenth Symposium (International) on Combustion, The Combustion Institute, pp. 401-407, 1974.

[2] S. Kumagai and H. Isoda, "Combustion of Fuel Droplets in a Falling Chamber", Proceedings of the Sixth Symposium (International) on Combustion, Reinhold, N.Y., pp. 726-731, 1957.

[3] H. Isoda and S. Kumagai, "New Aspects of Droplet Combustion", Proceedings of the Seventh Symposium (International) on Combustion, The Combustion Institute, pp. 523-531, 1959.

[4] C. H. Waldman, "Theory of Non-Steady State Droplet Combustion", Fifteenth Symposium (International) on Combustion, The Combustion Institute, pp. 429-442, 1974.

[5] S. Ulzama and E. Specht, "An Analytical Study of Droplet Combustion Under Microgravity: Quasi-Steady Transient Approach", Proceedings of the Thirty First Symposium (International) on Combustion, The Combustion Institute, pp. 2301-2308, 2007.

[6] I. K. Puri and P. A. Libby, "The Influence of Transport Properties on Droplet Burning", Combustion Science and Technology, Vol. 76, pp. 67-80, 1991.

[7] M. K. King and "An Unsteady-State Analysis of Porous Sphere and Droplet Fuel Combustion Under Microgravity Conditions", Proceedings of the Twenty Sixth Symposium (International) on Combustion, The Combustion Institute, pp.1227-1234, 1996.

[8] J. R. Yang and S. C. Wong, "An Experimental and Theoretical Study of the Effects of Heat Conduction through the Support Fiber on the Evaporation of a Droplet in a Weakly Convective Flow", Int. J. Heat Mass Transfer, Vol. 45, pp. 4589-4598, 2002.

[9] C. K. Law, "Multicomponent Droplet Combustion with Rapid Internal Mixing", Combustion and Flame, Vol. 26, pp. 219-233, 1976.

[10] R. B. Landis and A. F. Mills, "Effects of Internal Diffusional Resistance on the Vaporization of Multicomponent Droplets", Fifth International Heat Transfer Conference, Paper B7.9, Tokyo, Japan, 1974.

[11] C. K. Law, "Internal Boiling and Superheating in Vaporizing Multicomponent Droplets", AIChE Journal, Vol.24, pp. 626-632, 1978.

[12] A. Y. Tong and W. A. Sirignano, "Multicomponent Droplet Vaporization in a High Temperature Gas", Combustion and Flame, Vol. 66, pp. 221-235, 1986.

[13] P. Lara-Urbaneja and W. A. Sirignano, "Theory of Transient Multicomponent Droplet Vaporization in a Convective Field", Proceedings of the Eighteenth Symposium (International) on Combustion, The Combustion Institute, pp.1365-1374, 1980.

[14] J. W. Aldred, J. C. Patel, and A. Williams,

[15] Combust. Flame. 17 (2) (1971) 139-148.

[16] A. J. Marchese and F. L. Dryer, "The Effect of Liquid Mass Transport on the Combustion and Extinction of Bicomponent Droplets of Methanol and Water", Combustion and Flame, Vol. 105, pp. 104-122, 1996.

[17] C. K. Law and H. K. Law, "On the Gasification Mechanisms of Multicomponent Droplets", pp. 29-48, Modern Developments in Energy, Combustion and Spectroscopy, Pergamon Press, 1993.

[18] C. K. Law and H. K. Law, "A d^2 – law for Multicomponent Droplet Vaporization and Combustion", AIAA Journal, Vol. 20, No. 4, pp. 522-527, 1982.

[19] S. K. Aggarwal and H. C. Mongia, "Multicomponent and High-Pressure Effects on Droplet Vaporization", Transactions of ASME, Vol. 124, pp. 248-255, 2002.

[20] W. A. Sirignano "Fluid Dynamics and Transport of Droplets and Sprays", Cambridge University Press, 1999.

[21] S. L. Lerner, H. S. Homan, and W. A. Sirignano, "Multicomponent Droplet Vaporization at High Reynolds Numbers: Size, Composition, and Trajectory Histories", Seventy Third Annual AIChE Meeting, 1980.

[22] S. K. Aggarwal, Y. A. Tong, and W. A. Sirignano, "A Comparison of Vaporization Models in Spray Combustion", AIAA Journal, Vol. 22, No.10, pp. 1448-1457, 1984.

[23] B. D. Shaw, "Studies of Influences of Liquid-Phase Species Diffusion on Spherically Symmetric Combustion of Miscible Binary Droplets", Combustion and Flame, Vol. 81, pp. 277-288, 1990.

[24] M. Mawid and S. K. Aggarwal, "Analysis of Transient Combustion of a Multicomponent Liquid Fuel Droplet", Combustion and Flame, Vol. 84, pp.197-209, 1991.

[25] N. W. Sorbo, C. K. Law, D. P. Y. Chang, and R. R. Steeper, "An Experimental Investigation of the Incineration and Incinerability of Chlorinated Alkane Droplets", Proceedings of the Twenty Second Symposium (International) on Combustion, The Combustion Institute, p. 2019, 1989.

[26] C. K. Law, T. Y. Xiong, and C. H. Wang, "Alcohol Droplet Vaporization in Humid Air", Int. J. Heat Mass Transfer, Vol. 30, p. 1435, 1987.

[27] Y. Zeng and Chia-fon F. Lee, "Modelling Droplet Breakup Processes Under Micro-explosion Conditions", Proceedings of the Thirty First Symposium (International) on Combustion, The Combustion Institute, pp. 2185-2193, 2007.

[28] R. E. Sonntag, C. Borgnakke, and G. J. Wylen, "Fundamentals of Thermodynamics", Sixth Edition, John Wiley and Sons, 2003.

[29] Choi et al, "Ethanol Droplet Combustion at Elevated Pressures and Enhanced Oxygen Concentrations", AIAA, 41st Aerospace Sciences Meeting and Exhibit, Reno, Nevada, pp. 1-7, 2003.

[30] A. K. Agarwal, "Biofuels (alcohols and biodiesel) Applications as Fuels for Internal Combustion Engines", Progress in Energy and Combustion Science, Vol. 33, pp. 233-271, 2007.

[31] A. Srivastava and R. Prasad, "Triglycerides-Based Diesel fuels", Renewable and Sustainable Energy Reviews, Vol. 4, pp. 111-113, 2000.

[32] W. Yuan, A. C. Hansen, and Q. Zhang, "Predicting the Physical Properties of Biodiesel for Combustion Modeling", ASAE Transactions, Vol. 46(6), pp.1487-1493, 2003.

[33] L. D. Clements, "Blending Rules for Formulating Biodiesel Fuel", Biological System Engineering, University of Nebraska - Lincoln, NE 68583-07266, pp. 44-53, 1996.

[34] W. Yuan, A. C. Hansen, and Q. Zhang, "Vapour Pressure and Normal Boiling Point Predictions for Pure Methyl Esters and Biodiesel Fuels", Fuel, Vol. 84, pp. 943-950, 2005.

[35] C. Olikara and G. L. Borman, "A Computer Program for Calculating Properties of Equilibrium Combustion Products with some Application to I.C. Engines", SAE Paper 750468, SAE Trans, 1975.

[36] M. K. Jain, "Numerical Solution of Differential Equations", Second Edition, Wiley-Eastern Limited, 1984.

[37] C. K. Law and W. A. Sirignano, "Unsteady Droplet Combustion with Droplet Heating – II: Conduction Limit", Combustion and Flame, Vol. 28, pp.175-186, 1977.

[38] R. C. Reid, J. M. Prausnitz, and B. E. Poling, "The Properties of Gases and Liquids", Fourth Edition, McGraw Hill Book Company, 1989.